Simulation of fatigue debonding in adhesively bonded three-dimensional joint geometries using a cohesive zone model approach

F.Moroni
Centro Interdipartimentale Siteia.Parma, via G.P. Usberti 181/A, 43124 Parma

A.Pirondi, G. Giuliese
Dipartimento di Ingegneria Industriale, Università degli Studi di Parma, via G.P. Usberti 181/A, 43124 Parma

ABSTRACT. The cohesive zone model has been widely used for the description of quasi-static crack growth of interfaces and, recently, evolutions have been proposed in order to account for fatigue phenomena. In this work the cohesive zone model previously developed by the authors to simulate fatigue crack growth at interfaces in 2D geometries is extended to 3D cracks under mixed-mode I/II loading.

KEYWORDS. Fatigue crack growth simulation; Cohesive zone model; Abaqus.

INTRODUCTION

Composite materials and structural adhesive bonding showed their first applications in the aerospace industry, but thanks to continuous performance improvement and cost reduction, many more industry fields are approaching the use this type of materials. The extensive employment of composites requires a more and more sophisticated capability to simulate and predict their mechanical behaviour. For this purpose, analytical methods are being progressively integrated or replaced by the Finite Element Method. In engineering applications, fatigue life is one of the most important design issues and for the previously mentioned materials the fatigue life is related to the initiation and propagation of defects, which produce progressive adhesive debonding or composite material delamination.
This kinds of problem were historically studied using fracture mechanics where the kinetic of a fatigue crack was represented by a Paris-like equation which relates the range of strain energy release rate ΔG, to the crack growth da/dN:

$$\frac{da}{dN} = B\Delta G^d \tag{1}$$

In this simple approach the finite element method can be adopted by creating and running models with different crack lengths. For each analysis the value of the strain energy release rate can be obtained using the contour integral or the virtual crack closure technique (VCCT). Hence the number of cycles can be obtained by manually integrating the crack growth rate computed from the Paris law.
In some finite element softwares, this procedure is integrated in special features (i.e. *Debonding in Abaqus®). An alternative way for dealing with fatigue crack growth problems is using a cohesive zone model. This model was initially used to described the plastic zone at the crack tip in thin metallic sheets and later it has been used as a micromechanical model for the simulation of the quasi static crack growth problems, especially in the case of interface cracks such as delamination in composites and bonded joints [1-4]. The possibility to simulate the growth of a defect without any remeshing requirements and the relatively easy possibility to manipulate the constitutive law of the cohesive elements makes the cohesive zone model attractive also for the fatigue crack growth simulation. In the literature several works deal with this topic: Maiti and Geubelle [5], Roe and Siegmund [6] and Muñoz [7] defined models where the cohesive strength

is reduced using appropriate laws and parameters in a cycle by cycle approach. Turon et al [8] proposed instead a model where the calibration of cohesive parameter for cyclic loading is not required since a damage homogenization criterion is used for relating the experimental FCG rate with the damage evolution of the cohesive elements. Moreover a cycle-by-cycle FE analysis is not necessary for the integration of damage rate, which means a significant computational time saving. Using [8] as a reference, but modifying the damage definition, including an automatic strain energy release rate evaluation and introducing different mixed mode criteria for the computation of the fatigue crack growth rate, the authors developed a model able to correctly predict fatigue crack growth at interfaces in two-dimensional geometries [9,10]. In this work, the extension of the model to full 3D cracks undergoing mixed-mode I/II fatigue loading is presented, emphasizing especially the changes done with respect the 2D model.

DESCRIPTION OF THE 2D CZ MODEL

For the sake of brevity, only the most important features of the two-dimensional model are shown (the complete description can be found in the literature [9,10]). A triangular cohesive law is used (see Fig. 1) where s_{max} is the maximum stress, K_0 the initial stiffness and δ_C the critical opening. The fracture energy corresponds to the area underlying the cohesive law. The damage value D decreases the stiffness per unit area K with respect to the initial one, following the equation

$$K = (1 - D) K_0 \tag{2}$$

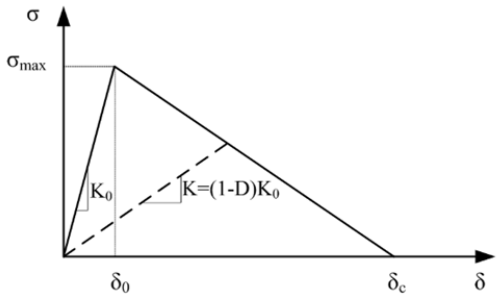

Figure 1: Cohesive law

Damage is representative of the effect of micro void nucleation and micro-cracks, therefore, considering a general Representative Surface Element (RSE) with a nominal surface equal to A_e, and a damaged area due to micro-voids or micro-cracks equal to A_d, D can be written [11]

$$D = \frac{A_d}{A_e} \tag{3}$$

Applying the equivalence criterion between damage and crack growth proposed in [8], damage increases with the number of cycles following Eq. 4, where A_{CZ} is the process zone area, evaluated by FE analysis on-the-run (see [9,10] for more detail).

$$\frac{dD}{dN} = \frac{1}{A_{CZ}} \frac{dA}{dN} = \frac{1}{A_{CZ}} B \Delta G^d \tag{4}$$

The procedure for the prediction of the crack growth rate has been implemented into the FE code ABAQUS using the embedded USDFLD subroutine to apply damage to the initial stiffness K_0. The simulation is carried out as a static analysis where a load equal to the maximum load of the fatigue cycle is applied. The strain energy release rate G is computed and then, using the cycle load ratio $R=P_{min}/P_{max}$, the strain energy release rate amplitude is calculated as

$$\Delta G = (1 - R^2) G \tag{5}$$

The value of ΔG is compared with the fatigue crack growth threshold ΔG_{th}. If $\Delta G > \Delta G_{th}$ the propagation will take place, otherwise the analysis is stopped and no propagation will occur. In the 2D model, at the beginning of each increment n,

the damage D_i^n in the cohesive elements belonging to the process zone A_{CZ} is increased by a given quantity $\Delta D_i^n = \min\{1-D_i^n, \Delta D_{max}\}$ where ΔD_{max} is a user-defined value. For each element lying in the process zone an increment in the number of cycles, ΔN_i^n is then estimated using Eq. 4 and the value of ΔG at that increment, ΔG^n. The routine searches for the minimum value among the calculated ΔN_i^n. This value, ΔN_{min}^n, is assumed to be the equivalent number of cycles of the increment. Then, the number of cycles is updated (N^{n+1}), and using again Eq. (4) the new damage distribution is computed for all the elements belonging to the process zone (D_i^{n+1}). The process zone is defined as where, during the analysis, the opening is higher than the maximum opening in the cohesive zone when the applied strain energy release rate is equal to the strain energy release rate threshold. Since the opening field ahead of the crack tip changes during crack propagation, the process zone area is continuously updated. It is worth to underline that the overall procedure is fully automated, i.e. the simulation is performed in a unique run without stops.

The ΔG at each increment is required in order to evaluate the crack growth rate. In 2D, G is evaluated through the calculation of the J-integral along a path Ω corresponding to the top and bottom nodes of the cohesive elements. With this choice, and neglecting geometrical nonlinearity, the J-integral reduces to:

$$J = \int_{\Omega} \left(-\sigma_{12} \frac{\partial u_1}{\partial x_1} - \sigma_{22} \frac{\partial u_2}{\partial x_1} \right) d\Gamma \tag{6}$$

Extracting the opening/sliding and the stresses in the cohesive elements at the beginning of the increment, the strain energy release rate is then computed. An interesting feature of this approach is that the mode I and the mode II component of the J-integral can be obtained by integrating separately the second or the first components of the integral in Eq.(6), respectively. Under mixed-mode I/II loading conditions, the parameters B and d of Eq. (1) are a function on the mixed mode ratio $MM = G_{II}/(G_I + G_{II})$ according to the Kenane and Benzeggagh model [12] as given by the following two equations:

$$d = d_1 + (d_2 - d_1) \cdot (MM)^{m_d} \tag{7}$$

$$\ln B = \ln B_2 + (\ln B_1 - \ln B_2)(1 - MM)^{m_B} \tag{8}$$

where d_1, B_1 and d_2, B_2 are, respectively, the parameters under pure mode I and pure mode II, and m_B and m_d are material parameters.

EXTENSION OF CZ MODEL TO 3D GEOMETRIES

For 3D simulation, the framework of 2D model in maintained, while the calculation of ΔG must be done at different locations along the crack front in order to account for 3D effects.

The J-integral method shown above can be easily implemented for a two-dimensional problem, since there is only one possible path. In the case of three dimensional problem the implementation is more difficult since several paths can be identified along the crack width, and moreover their definition is rather troublesome, especially when dealing with irregular meshes. In this work, the cohesive zone is meshed with a regular grid equally sized brick cohesive elements, therefore Eq. 6 can be computed on parallel contours along the crack front, each contour pertaining to a row of cohesive elements across the crack front. The damage rate dD/dN can be therefore different along the crack front depending on the J-value.

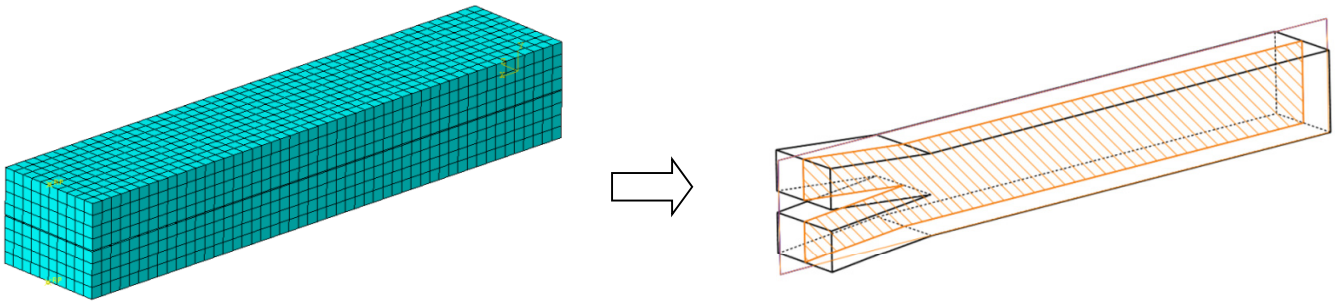

Figure 2: The 3D geometry is reduced to 2D slices, each one pertaining to a row of cohesive elements.

A 3D model is therefore considered as a sequence of slices, each one analysed as a 2D model (Fig. 2).

FE MODELS

The model geometries are illustrated in Fig. 3, while the material properties, the applied load, the cohesive law parameters, the specimens dimension and the Paris law equation coefficients are shown in Tab. 1.
The mesh size in the adherends is 1 mm, while in the cohesive layer it is reduced to 0.5 mm. For all the simulation a load ratio R = 0 is assumed.

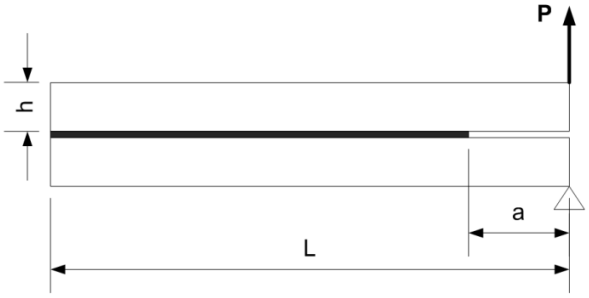

Mode I - DCB

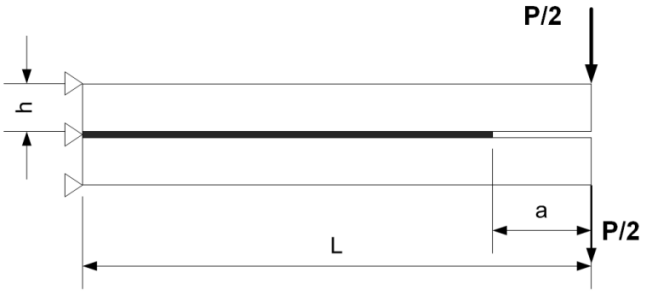

Mode II - ELS

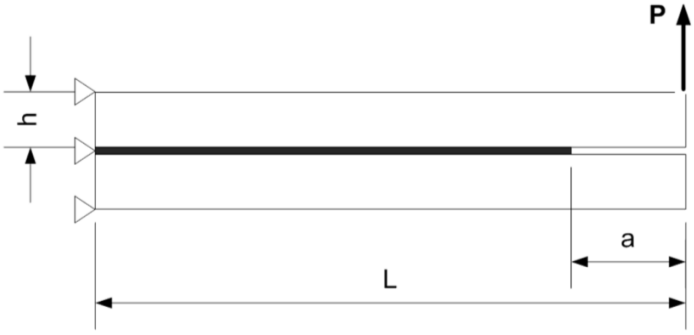

Mixd mode I/II – MMELS

Figure 3: Geometries simulated.

Young's Modulus	E [MPa]	70000
Poisson's ratio	ν	0.25
Applied load	P [N]	100
Mode I Cohesive energy	Γ_I[N/mm]	0.26
Mode II Cohesive energy	Γ_{II}[N/mm]	1.002
Mode I Cohesive strength	σ_{max_I} [MPa]	30
Mode II Cohesive strength	σ_{max_II} [MPa]	30
Initial stiffness of cohesive law	K_0[MPa/mm]	10000
Mode I critical opening	δ_{C_I} [mm]	0.0173
Mode II critical opening	δ_{C_II} [mm]	0.067
Specimen length	L [mm]	50
Specimen width	b [mm]	10
Specimen thickness	2h [mm]	8
Initial crack length	a_0 [mm]	10
Paris law coefficient	B	0.5
Paris law exponent	d	3
KB parameter	m_d	1.85
KB parameter	m_B	0.35

Table 1: Material properties [8, 12].

RESULTS

In order to verify the accuracy of the model, two comparison are made:
- the estimation of G during the crack growth is compared with the reference trend obtained using the VCCT method on an equivalent 2D plane strain model (the 3D innermost path is taken for comparison)
- the crack growth rate obtained by the simulation as a function of the range of applied strain energy release rate is compared with the crack growth rate given in input.

These same comparisons are made for the DCB (Fig. 4 - MM=0), ELS (Fig. 5 - MM=1) e MMELS (Fig. 6 - MM=0.4) geometry. Moreover for the MMELS geometry the trends of the strain energy release rate and of the Mixed mode ratio is evaluated along the joint width (Fig. 7).

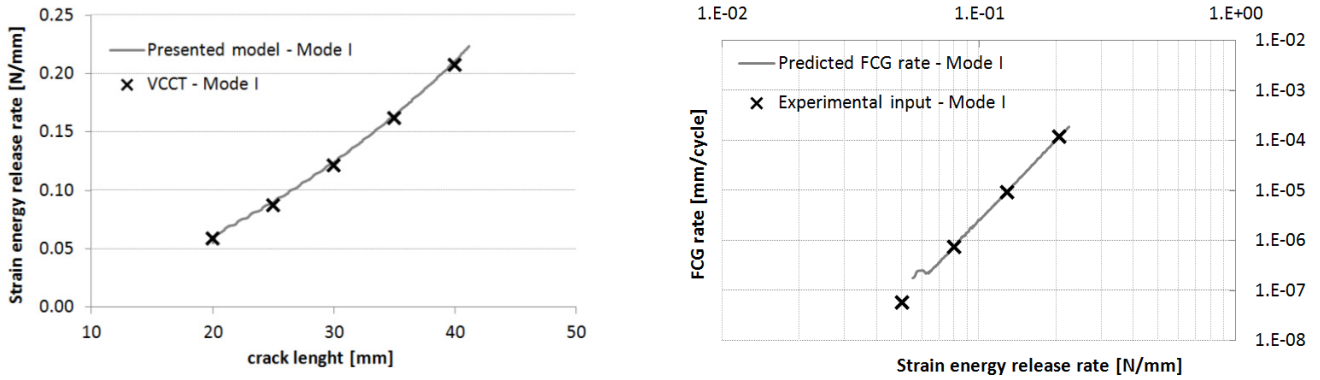

Figure 4: Comparison between reference trends and the results of the simulation for the trend of G and the crack growth rate; DCB geometry.

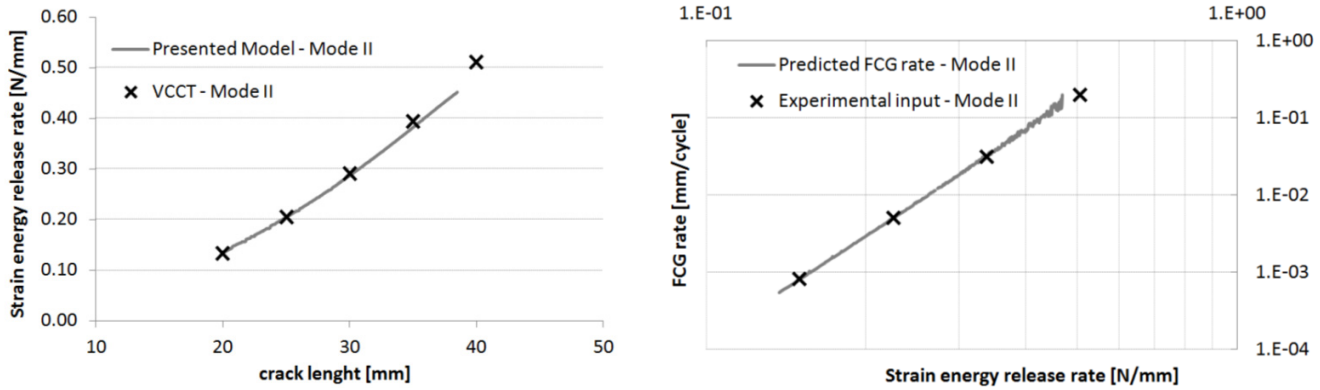

Figure 5: Comparison between reference trends and the results of the simulation for the trend of G and the crack growth rate; ELS geometry.

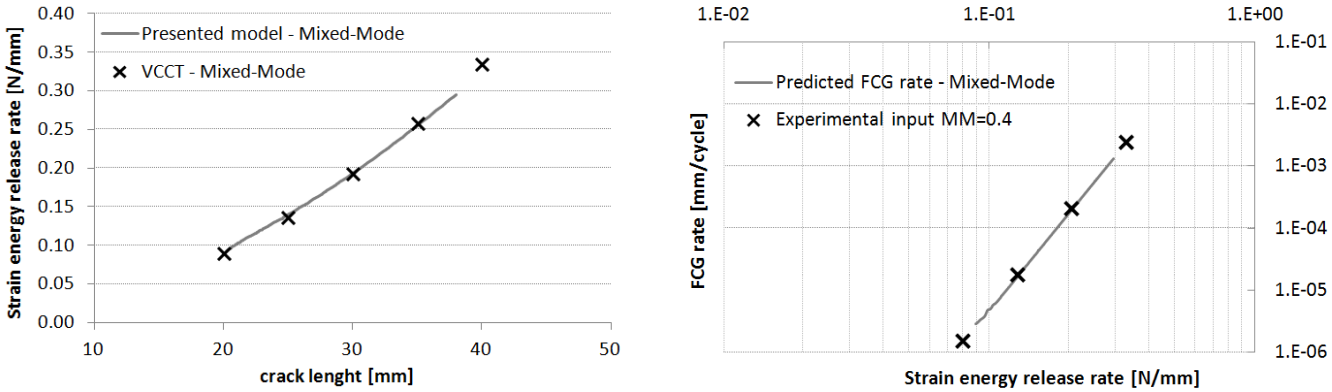

Figure 6: Comparison between reference trends and the results of the simulation for the trend of G and the crack growth rate; MMELS geometry.

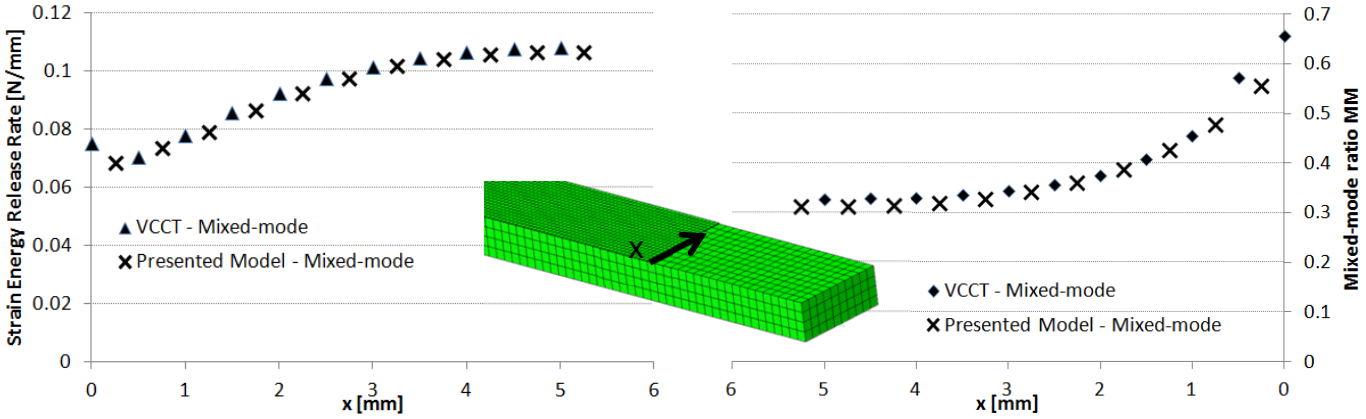

Figure 7: Comparison between VCCT and result of simulation for the trends of G and MM along the joint width.

All the comparisons in good agreement with the input values. Moreover since the G-value can change along the joint width, different crack growth rates can be displayed, leading to a curved crack front. For example in the DCB simulation, when stable propagation is reached, the crack is longer in the mid-plane with respect to the outer bound. This is qualitatively in good agreement with experimental observation coming from DCB crack propagation tests (Fig. 8).

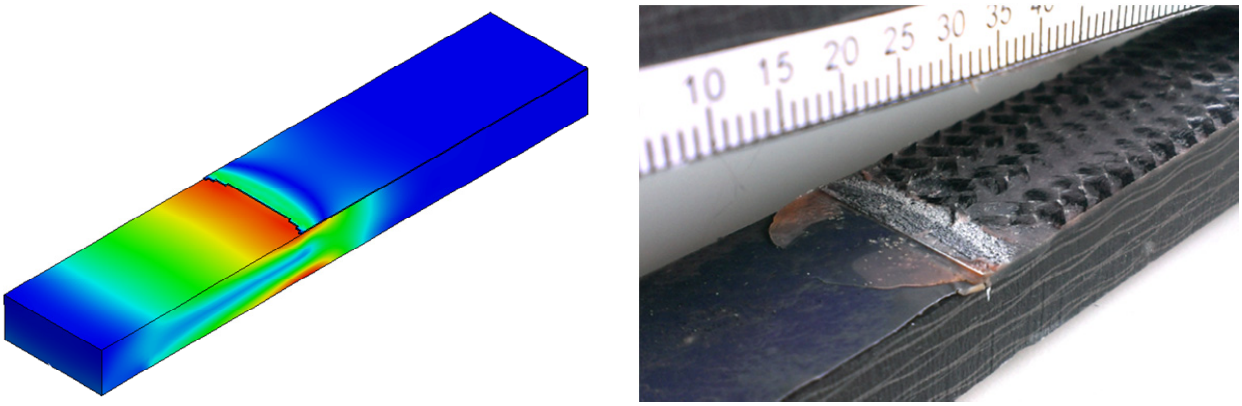

Figure 8: Qualitative comparison of the crack front shape between simulation and experimental fatigue DCB tests.

CONCLUSIONS

In this work an initial extension to 3D of the 2D cohesive zone model developed in [10] has been presented. The result are compared with reference trends (VCCT and/or analytical) and a good agreement is found.
Future developments will involve the definition of a procedure able to compute the strain energy release rate without any requirements on the mesh shape.

REFERENCES

[1] G. Barenblatt, Advanced Applied Mechanics, 7 (1962) 55.
[2] J. W. Hutchinson, A. G. Evans, Acta Materialia, 48 (2000) 125.
[3] B.R.K. Blackman, H. Hadavinia, A.J. Kinloch, J. G. Williams, International Journal of Fracture, 119 (2003) 25.
[4] S. Li, M. D. Thouless, A.M. Waas, J. A. Schroeder, P.D. Zavattieri, Composite Science and Technology, 65 (2005) 281.
[5] S. Maiti, P. H. Geubelle, Engineering Fracture Mechanics, 72 (2005) 691.
[6] K. L. Roe, T. Siegmund, Engineering Fracture Mechanics, 70 (2003) 209.
[7] J. J. Muñoz, U. Galvanetto, P. Robinson, International Journal of Fatigue, 28 (2006) 1136.

[8] A. Turon, J. Costa, P.P. Camanho, C.G. Dávila, Composites, 38 (2007) 2270.
[9] A. Pirondi, F. Moroni, International Journal of Adhesion & Adhesives, 29 (2009) 796.
[10] F. Moroni, A. Pirondi, Engineering Fracture Mechanics, 89 (2012) 129.
[11] J. Lemaitre, Journal of Engineering Materials and Technology, 107 (1985) 83.
[12] M. Kenane and M. L. Benzeggagh, Compos. Sci. Technol., 57 (1997) 597.